

Trapping and detrapping of electrons photoinjected from silicon to ultrathin SiO₂ overlayers. II. In He, Ar, H₂, N₂, CO, and N₂O

N. Shamir^{a)} and H. M. van Driel^{b)}

Department of Physics, University of Toronto, Toronto, Ontario M5S 1A7, Canada

(Received 5 January 2000; accepted for publication 15 April 2000)

Photon-induced gas-assisted charging (PIGAC) of 1.5 nm thick SiO₂ overlayers by photoemission from the Si substrate is demonstrated to be a universal feature for all gases. In our case (multi)photoemission is induced by high-intensity 800 nm, 150 fs pulses in samples at 295 K. O₂ is more effective than other gases, probably due to the accumulation of surface charge following the formation of O₂⁻ on the surface. For the other gases, the efficiency decreases with increasing molecular (or atomic) size, pointing to a mechanism that is dependent on the proximity of the gas molecules to charge traps. Combined measurements of photoemission current and the contact-potential-difference detected charge spillover from the irradiated spot to the rest of the surface. Transfer of PIGAC electrons to long-lifetime charge traps was also detected for all gases. Its efficiency is the highest for He, probably due to the larger effective surface (and thus larger PIGAC) created by He penetration into the oxide layer. Detrapping of trapped electrons also occurs with PIGAC, and is particularly effective for CO and H₂. Its mechanism and gas specificity are not understood as yet, but the strong increase of detrapping with decreasing temperature suggests a dependence on longer proximity of the gas molecules to the traps due to an increased surface residence time. © 2000 American Institute of Physics. [S0021-8979(00)05214-2]

I. INTRODUCTION

The trapping and redistribution of charges in the Si/SiO₂ system are important in fundamental and applied research. In a previous publication,¹ henceforth paper I, laser-induced charge redistribution and trapping were studied in detail for clean Si(001) and the Si(001)/SiO₂ system (for an oxide thickness <1.5 nm) both in vacuum and in an O₂ ambient gas. Charge transfer was induced by internal photoemission following single- or multi-photon absorption of 200 fs, 800 nm (1.55 eV), pulses in the Si with peak power ≲30 GW/cm². Surface charging and redistribution were observed via changes in the work function monitored via external multiphoton photoemission (MPPE) or contact potential difference (CPD) techniques using a Kelvin probe.² It was shown that charging of the oxide or Si/SiO₂ interface can occur via direct filling of oxide or Si interface traps in the absence of O₂. No lateral redistribution of trapped charges was detected on a laboratory time scale. Diversity, both in the initial photoemission-current and with some correlation to the size of the DF effect, is attributed to variation in the initial density of charge traps and populations.

When O₂ gas was introduced at various pressures $P < 30$ Torr, and the surface is illuminated, two additional processes occur. Three photon-photoemission electrons are injected into the SiO₂ (or to the clean Si) surface and combine with the O₂ molecules to transiently charge the surface. The charge density is proportional to $\log(P)$ in agreement with the Fowler–Guggenheim isotherm³ for mutual repulsing ad-

sorbates. The maximum charge density (measured by second harmonic generation, SHG) is estimated as⁴ $\sim 10^{13}$ cm⁻². The surface charge is efficiently transformed into a second gas-sensitive family of traps as well as to the direct filling traps, with a maximum charge density of $\sim 10^{12}$ cm⁻².⁴ The gas-sensitive family is present only in the oxide and their filling is significantly more efficient than the direct filling process.

From electric-field-induced second harmonic generation measurements⁵ it was initially suggested that O₂ was unique as a gas in either initiating or maintaining surface charging of Si/SiO₂ samples (with thin oxide layers), at least for $P > 1$ Torr, below which the technique was not sensitive. However, measurements of the CPD following adsorption of He, Ar, H₂, N₂, and CO gave signatures of the same sign, similar magnitude,⁶ and a $\log P$ dependence for all gases. This unusual similarity was also observed for PIGAC through MPPE experiments and explained by a universal mechanism of electrostatic coupling of the adsorbed species to the negative charges residing on the SiO₂ surface. It was suggested that the electrostatic coupling mutually traps the adsorbed species and the internally photoemitted electrons, thereby inducing the transient surface charging. Oxygen was still found to be a special case in that strong surface charge accumulation follows the first step of surface charging (common to all gases). It was suggested that an adsorbed O₂ molecule combines with a transiently trapped surface electron to form metastable O₂⁻ (molecular chemisorption) on the surface.⁴ Spillover of the transient surface charge from the laser-irradiated spot to the whole surface area (probably due to Coulomb repulsion) was observed for all the studied gases.

^{a)}Permanent address: Nuclear Research: Center-Negev, P.O. Box 9001, Beer-Sheva, Israel.

^{b)}Corresponding author; electronic mail: vaudriel@physics.utoronto.ca

In the present paper, details of the PIGAC mechanism in the presence of He, Ar, H₂, N₂, CO, and N₂O and charge transfer to long-lifetime traps are presented for the Si/SiO₂ system as well as clean Si samples. Also, a gas-assisted (temperature dependent) detrapping effect is presented and discussed.

II. EXPERIMENTAL DETAILS

The overall experimental setup including details of the 200 fs, 800 nm laser, the vacuum system, the Kelvin probe for making CPD measurements, and MPPE techniques are described in paper I. For simplicity, as in paper I, we define a normalized photoemission current, I_c , which is referenced to a previously unexcited (virgin) region of a sample. A change in the photocurrent can be related to a change in the work function, $\Delta\Phi$.

All samples were taken from polished, optically smooth Si(100) wafers and had a surface area of $\sim 2 \times 12 \text{ mm}^2$ and thickness of 0.3 mm. The samples used were part of the list given in paper I: (a) 15Sn: a $\sim 15 \text{ \AA}$ oxide film grown in steam at 850 K on a low-doping *n*-Si(001) substrate [resistivity 20–100 ($\Omega \text{ cm}$)]; (b) 10Ap: a 10 \AA oxide layer produced by anodic oxidation using 0.1 M HCl with a low-doping [resistivity 3–7 ($\Omega \text{ cm}$)] *p*-Si(001) substrate; (c) CLn: the oxide of a 15Sn sample was removed (in UHV) by resistive heating at 1400 K (cleanliness checked by *in situ* Auger electron spectroscopy); (d) CLp: a 10Ap sample, the oxide of which was removed by the same method as in (c). Both clean Si surfaces were passivated by a long exposure to oxygen (forming a chemisorbed layer), so further gas admission resulted in reversible CPD values. The gases used in the experiments were either research grade (99.9999%) or ultra-high purity (99.999%) quality. To rule out water vapor effects, a cold trap was used in the gas admission line but found not to alter the experimental results.

III. RESULTS

A. Photoemission current and CPD measurements of gas exposures

Measurements of I_c during illumination plus exposure of a 15Sn sample to 0.1 Torr of four gases are depicted in Fig. 1. Following the gas exposure, I_c drops for all gases, and more so for the heavier gases. While the reduction seems to be time independent for H₂ and CO, for O₂ there is a strong accumulation effect, as noted in paper I. For He, a continuous decrease is observed and can be explained through the difference in adsorption characteristics of O₂ and He as depicted in Fig. 2 and discussed below. Combined I_c and CPD measurements during exposure of a 15Sn sample to 1 Torr He and H₂ are presented in Figs. 3 and 4, respectively. The presence of the Kelvin probe somewhat affects the absolute value of the photoemission current but not its functional behavior.

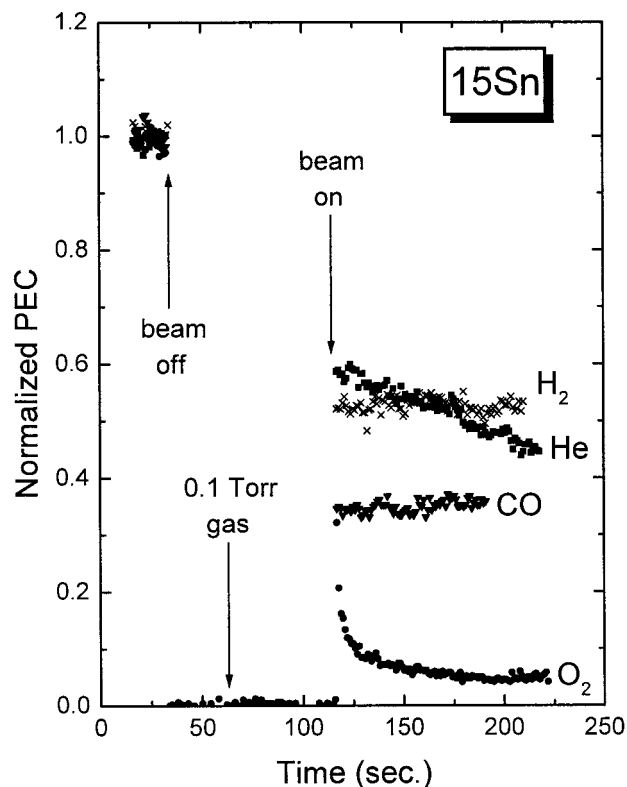


FIG. 1. Photoemission current measurement sequences of Si/SiO₂ (15Sn sample) before, during and following exposure to 0.1 Torr of He, H₂, CO, and O₂.

B. Residual photoemission current following gas pumping

Figure 5 presents three typical gas exposure, photoemission current sequences on a 15Sn sample, including the residual current measured after the gas was pumped out. The pressure dependence of the current decrease is well exhibited for H₂. For all gases, the residual current is lower than the initial value, the reduction being gas specific and pressure dependent. Figure 6 presents current measurements of a He 1 Torr exposure sequence on 15Sn and CLn samples. While the initial decrease, following gas exposure is sample independent, the subsequent decrease is much stronger for 15Sn and its residual current is significantly lower. The exposure plus illumination sequence of 1 Torr He on a 15Sn sample for 300 K and 200 K is presented in Fig. 7. At least for these temperatures the process seems to be temperature independent (in contrast to the O₂ case¹).

In some cases, particularly for H₂ and CO, the residual current (and in rare cases also the photoemission current following exposure) is higher than its initial value. Figure 8 presents three such cases. When CO is used on a 15Sn sample and is removed, the residual current is higher than the initial value. A time-dependent decrease, typical of the direct filling process (see paper I), occurs. When a direct filling-saturated spot is exposed to 0.02 Torr of H₂ on the same sample, the current immediately following exposure is higher than the initial (vacuum) value and the residual current returns to its initial value. The bottom frame of Fig. 8 depicts a combined series of He and H₂ exposures on a spot

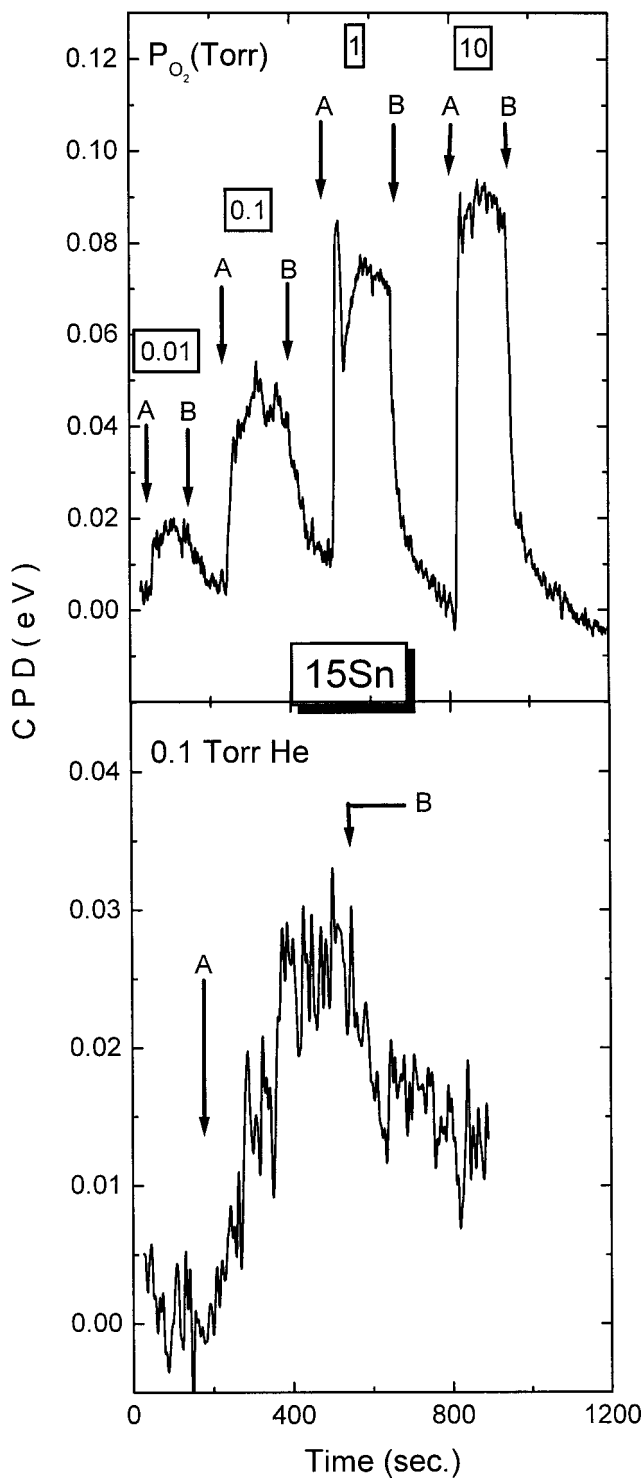


FIG. 2. The CPD measurement of O₂ and He physisorption and desorption on a 15Sn sample. A—gas admission; B—pump-out.

previously exposed to 0.002 Torr O₂. First, 30 Torr He is applied and, after removal, the residual current is lower than the initial value (as expected the residual current for 0.002 Torr O₂ is far from saturation: see paper I). Following a 30 Torr H₂ exposure on the same spot, however, the residual current after removal is significantly higher than both the last residual and initial current. Also the direct-filling-like, time-

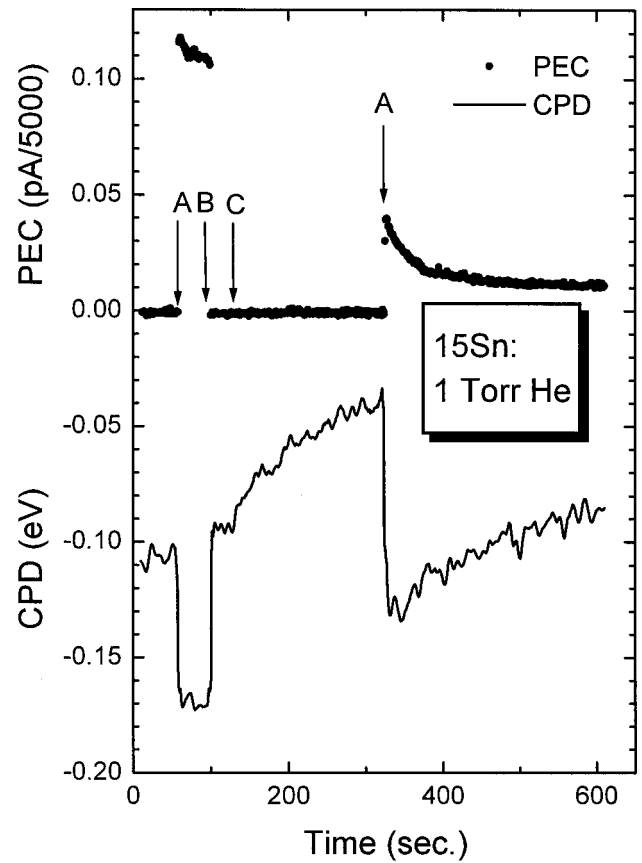


FIG. 3. Combined CPD and photoemission current measurement of the exposure of a 15Sn sample to 1 Torr He. A—beam off; B—beam on; and C—gas admission.

dependent decrease occurs again. A significant temperature effect on the detrapping process is demonstrated in Fig. 9, which illustrates four exposure plus illumination sequences for H₂. For (a) 0.01 Torr, the current initially increases with exposure, in contrast to the usual behavior. Also the residual PEC is higher than the initial value. For (b), 0.1 Torr, the initial current is higher and the initial decrease with exposure is significantly smaller than for 300 K (see Fig. 1). After pumping the residual current is again higher than the initial value and a strong direct-filling process seems to occur. The same trend is depicted in (c), 1 Torr. The current, following the initial decrease with exposure, increases. After pumping, the residual current is again higher and direct filling is significant. The fourth sequence, (d), is a 0.01 Torr exposure following the (c) 1 Torr sequence. The initial current is significantly higher, but the exposure+illumination sequence seems to be normal again.

IV. ANALYSIS AND DISCUSSION

A. Photon-induced gas-assisted (surface) charging

The changes in the current amplitude due to gas introduction, depicted in Fig. 1, reflect the value of $\Delta\Phi$ that for oxygen was established to be caused by three photon emission charging of the surface.⁵ The cumulative effect for oxygen (that indeed has a time dependence similar to that observed for electric-field-induced second harmonic

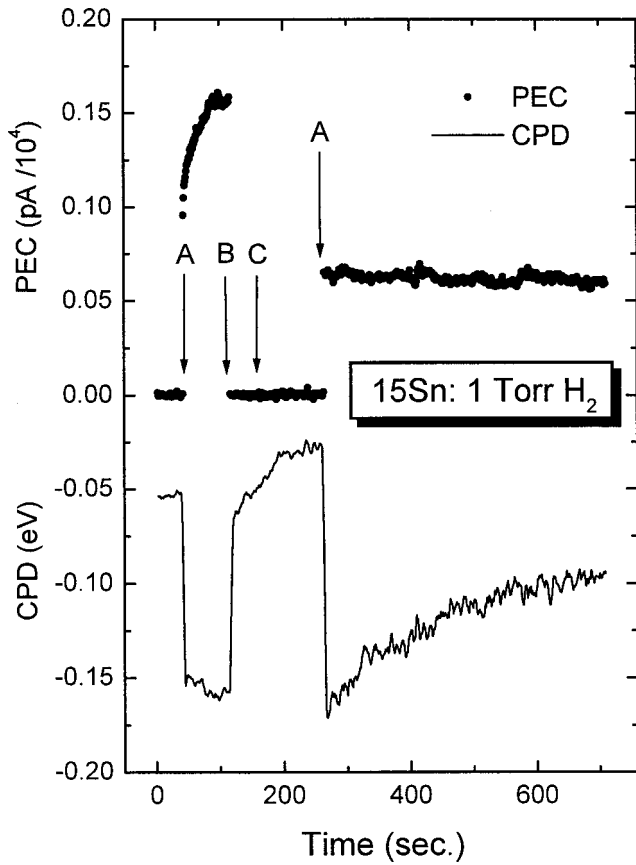


FIG. 4. Combined CPD and photoemission measurement of the exposure of a 15Sn sample to 1 Torr H₂. A—beam off; B—beam on; and C—gas admission.

generation⁴) is therefore explained by accumulation of surface charge, while for the other gases a steady-state surface charge is reached immediately. As can be observed in Fig. 2, the adsorption and desorption times of He are significantly longer than those of O₂, probably indicating penetration into the oxide bulk. The continuous decrease of the current for He (Fig. 1) is therefore due to the increase of the work function of the surface that is being charged by the photoelectrons.

Figure 10 presents the pressure-dependent $\Delta\Phi$ due to adsorption for He, Ar, H₂, O₂, N₂, CO, and N₂O as measured with the Kelvin probe. As noted earlier,⁶ the similarity of the changes in magnitude and sign is unusual assuming regular physisorption. This led us to the proposal of electrostatic adsorption. Figure 11 shows the initial decrease in PEC versus pressure for the same gases where the relative PEC changes have been expressed in terms of $\Delta\Phi$ according to Eq. (2) (the calibration of the $\Delta\Phi$ scale is discussed later). Similarly to Fig. 10, the pressure dependence in Fig. 11 is of the form $\Delta\Phi = a + b \log(P)$ for all the gases, where a and b are constants. All the $\Delta\Phi$ versus P slopes, except that for oxygen, converge to $\Delta\Phi = 0$ at $P \sim 1-2$ Torr. Furthermore, the heavier gases have stronger pressure dependence and higher $\Delta\Phi$ values.

The pressure dependencies of $\Delta\Phi$ for various gases in Fig. 11 are different than that of Fig. 10, and also for most of the gases the effect is larger than that of oxygen (compared to that presented in Fig. 10). This still does not prove that

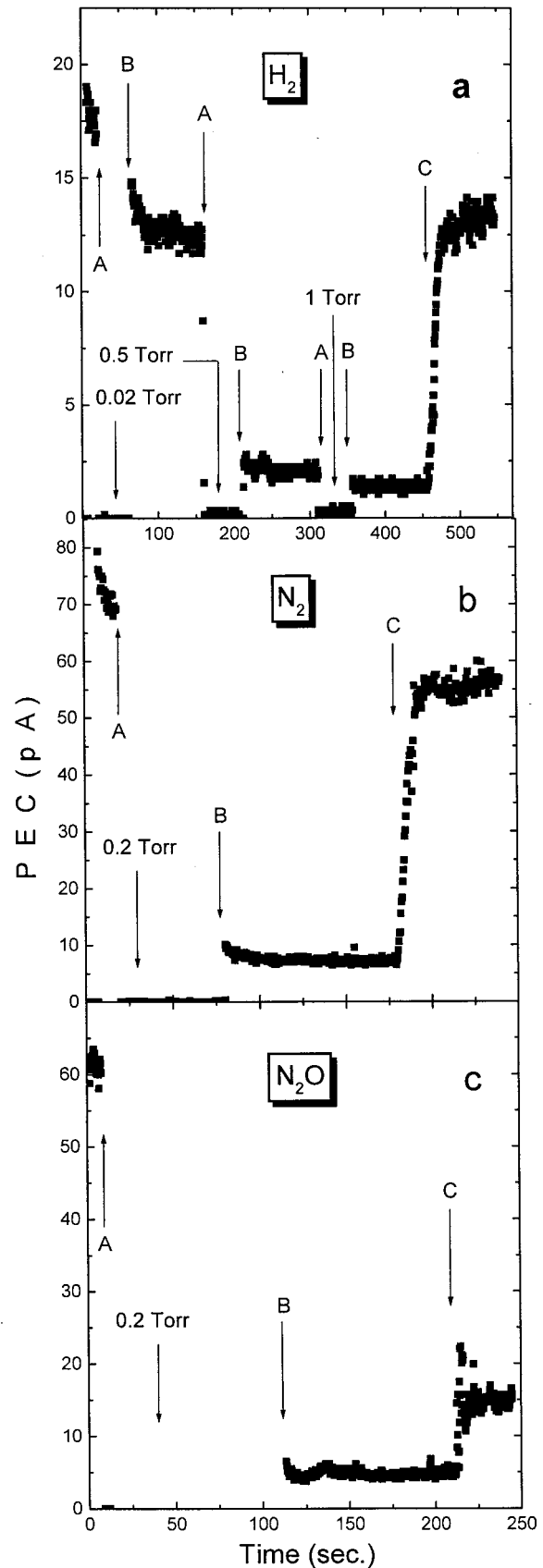


FIG. 5. Photoemission current measurement sequences on a 15Sn sample before, during and following exposure to gases. A—beam on; B—beam off; and C—gas pump-out.

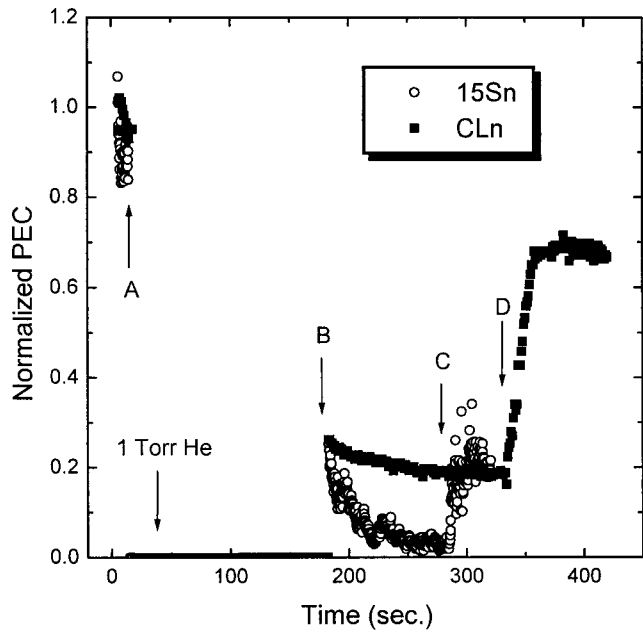


FIG. 6. Photoemission current measurement sequences of exposure of 15Sn and CLn samples to 1 Torr He. A—beam off; B—beam on; C—pump-out for 15Sn; and D—pump-out for CLn.

photo-induced gas-assisted charging occurs, since the measurement of net gas adsorption under beam irradiation may be different (photon-assisted effects, elevated temperature) than the one measured by the Kelvin probe (Fig. 10). To check independently whether gas-assisted charging of the surface occurs for other gases besides O₂, for which its occurrence has been established,^{5,7} combined photocurrent and CPD measurements were performed for different gases and pressures. It has to be noted that the ratio of the area monitored by the Kelvin probe (2.5 mm diameter) and that affected by the laser beam is ~10³. The probe is therefore

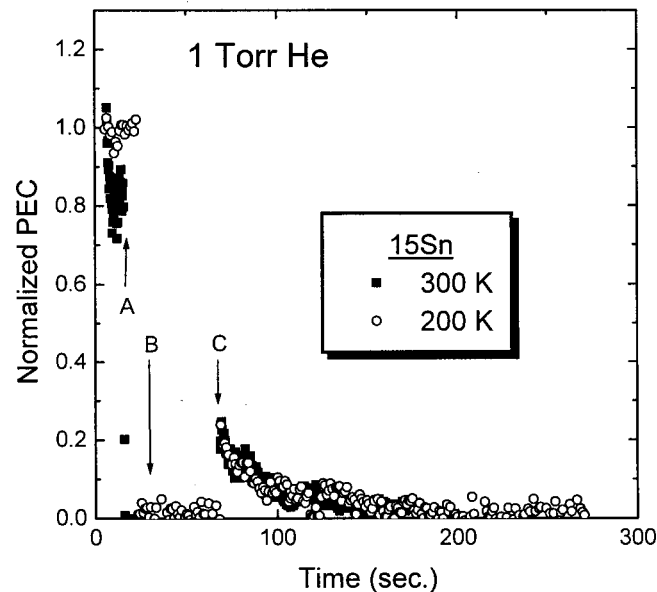


FIG. 7. Photoemission measurement sequences of exposure of 15Sn to 1 Torr He at 200 K and 300 K. A—beam off; B—gas introduction; and C—beam on.

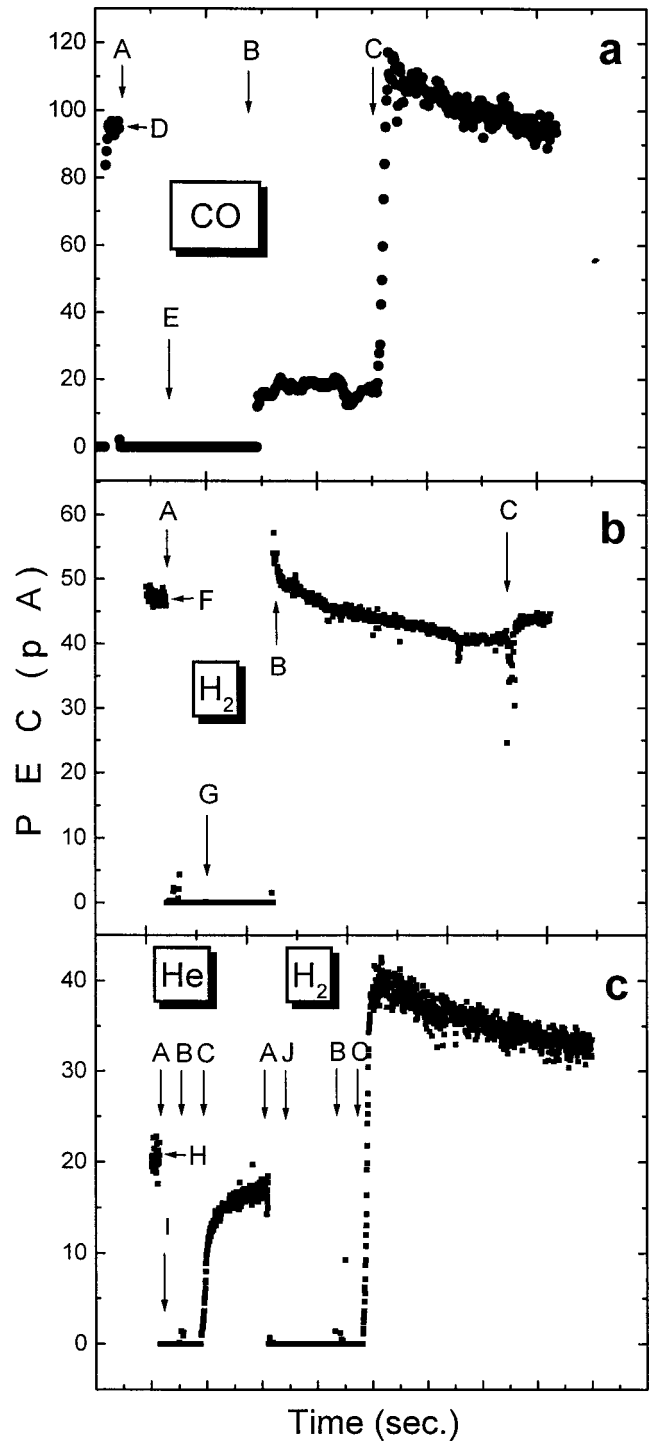


FIG. 8. Three examples of gas-assisted detrapping at a 15Sn surface. A—beam off; B—beam on; C—gas pump-out. (a) D—virgin-photoemission current; E—admission of 0.3 Torr CO; (b) F—direct filling saturated current; G—0.02 Torr H₂. (c) H—0.002 Torr O₂ exposure, residual current; I—30 Torr He; J—30 Torr H₂.

insensitive to processes that are confined to the laser-affected spot area even when the latter is monitored by the probe. Hence, and also in order to ensure that there is no direct interaction of the probe with the laser beam, the irradiation spot was located ~1 mm away from the edge of the probe-monitored area.

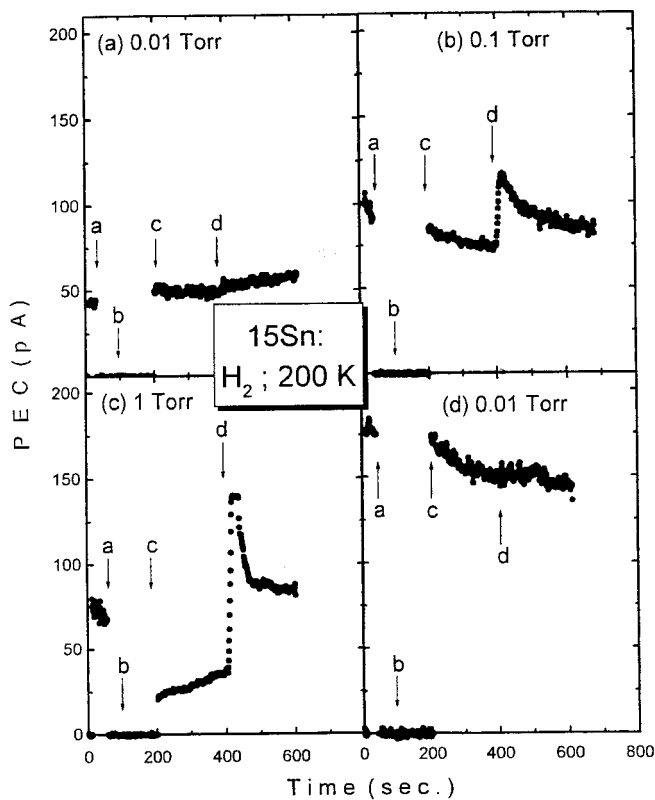


FIG. 9. H_2 assisted gas detrapping at a 15Sn surface at 200 K: four consecutive gas+laser illumination sequences. a—beam off; b—gas admission; c—beam on; and d—gas pump-out.

In Figs. 1, 3, and 6, for He exposure on 15Sn, the beam was turned on before the He penetration into the oxide ended (see Fig. 2) and hence the continuous decrease in photoemission current. But clearly, at about 500 s, when the current no longer changes with time, the CPD continues to rise. For H_2

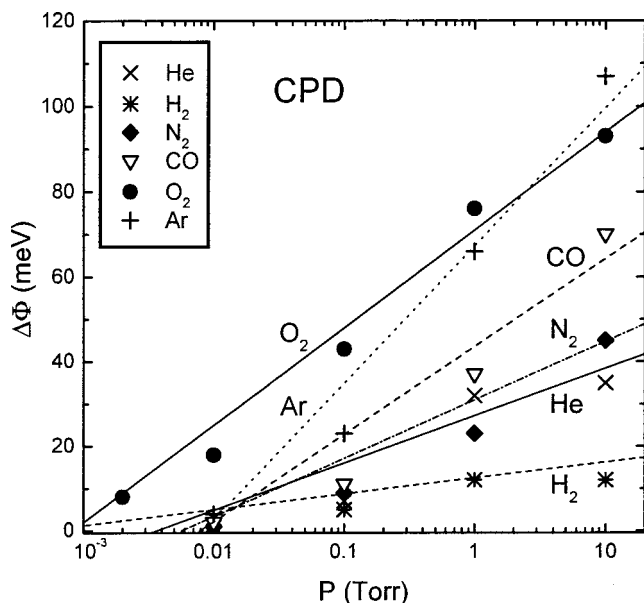


FIG. 10. The CPD measurement of the physisorption of the various gases versus ambient gas pressure. The line for each gas is the best fit for the experimental data.

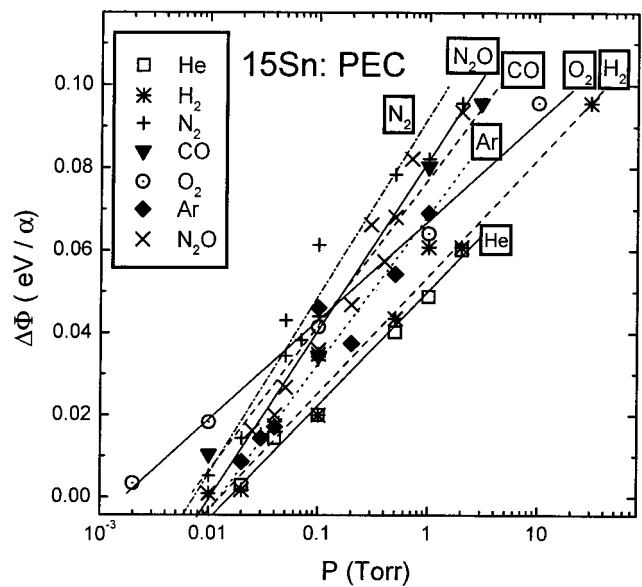


FIG. 11. The initial photoemission current decrease translated into $\Delta\Phi$ (scaling discussed in the text) as a function of ambient gas pressure for all gases studied. The line for each gas is the best fit for the experimental data.

in Fig. 4, it is more obvious. The clear continuous increase of the CPD, although the photocurrent is constant due to an immediately reached steady state, indicates the occurrence of photo-induced gas-assisted charging. As indicated above, the Kelvin probe is sensitive to such a process only if charge spreads outside the irradiated spot (spillover). It is therefore concluded that some of the photo-induced surface charge moves from the irradiated spot, probably due to Coulomb repulsion, to a wide area (probably the whole surface). Since no lateral resolution is available in the experiments, no quantitative relation between the measurement depicted in Fig. 4 and the CPD change in the irradiated spot can be obtained. Changing the distance between the laser spot and Kelvin probe-monitored area did not yield significantly different results. The charge accumulation, monitored by the CPD measurement, is higher for higher photoemission current (and therefore internal photoemission) intensities.

Assuming that the difference between Figs. 10 and 11 results only from photo-induced gas-assisted charging, the factor (unknown, but >1 as demonstrated by the spillover measurement for O_2 , Fig. 11 of paper I) by which the initial O_2 -induced photoemission current signal exceeds that of adsorption alone is taken to be α . The direct filling scale of Fig. 11 is therefore calibrated as $\alpha\Delta\Phi$ of Fig. 8 by equalization of the two best fit curves for O_2 .

From a comparison of Figs. 10 and 11, it seems that, except for He and Ar, surface charge trapping of the other gases is actually more effective than for oxygen. Of course, as noted above, these differences may be, at least partly, due to the different physisorption conditions for the cases depicted in the two figures. In any case, the fact that, for every gas, the pressure dependence (up to a constant factor) is the same for physisorption and photo-induced gas-assisted charging means that the surface transient charge is proportional to the number of adsorbed species. This is in accor-

dance with the mutual electron-gas attachment on the surface, so that the internally photoemitted electrons transiently trap additional gas species. The inability to measure the net adsorption with and without the irradiation effect makes it impossible to determine the gas-assisted charging efficiency for the different gases.

In contrast to the electrostatic adsorption by fixed surface charge,⁶ Coulomb repulsions cause spillover of nonfixed electrons from the irradiated spot, as measured by the KP (Figs 3 and 4). When a steady state is achieved between charging and spillover (and assuming no significant transfer to long-living charge traps), no decrease is observed for the current after the initial gas-induced one (H_2 and CO in Fig. 1). Transient surface charge accumulation and effective enlargement of the surface result in a further decrease of the photoemission (O_2 and He). Photo-induced gas-assisted charging is a common phenomenon to all studied gases, including O_2 . Therefore, the formation of an O_2^- species, which makes O_2 a special case of high charge accumulation on the surface,¹ probably occurs in a later step, following gas-assisted charging and not by “harpooning” as suggested earlier.

The amount of charge spillover is qualitatively controlled by the photoemission current amplitude and to a much lesser extent by the gas pressure (for 10 Torr the transfer is about the same as for 1 Torr). This may reflect that spillover consists of coupled electron-gas dipoles, a movement that occurs less rapidly for a denser adsorbed layer. Typically spillover accumulation induces a $\Delta\Phi=0.005$ to 0.01 eV (Fig. 4). For a 1.6 nm oxide the maximum near-interface electric field is (assuming it is across the oxide) ≈ 0.6 MV/cm. Taking the oxide dielectric constant to be $\epsilon_r=3.8$, we estimate from Gauss’s law that the surface charge density is $\sim 5 \times 10^{11} \text{ cm}^{-2}$.

It is interesting to note that the He exposure+illumination sequence seems to be identical for 200 K and 300 K. In addition to implications for detrapping, discussed in Sec. IV C, this has to be compared to the distinct difference between the 200 K and 300 K sequences for O_2 (Fig. 7 of paper I). This points to the special mechanism of charge accumulation for O_2 assumed to be by the formation of O_2^- on the surface⁷ following the adsorption. The maximum in charge accumulation was suggested¹ to be a result of two potential wells for dissociative chemisorption, related to electrostatically adsorbed² O_2 and surface⁷ O_2^- .

B. Charge trapping

In paper I, a model was proposed in which there is a transfer from the photo-induced gas-assisted surface charge to charge traps in the oxide as well as in the Si bulk. The reduction in current from the initial to the residual value represents the fraction of charge transferred to traps. It was also demonstrated for oxygen that, in the silicon bulk, the charge traps are those that are also directly filled by photoelectrons. On the other hand, those traps that are exclusively filled by transfer from gas-assisted charging (and therefore sensitive to the presence of ambient gas) are present only in the oxide.

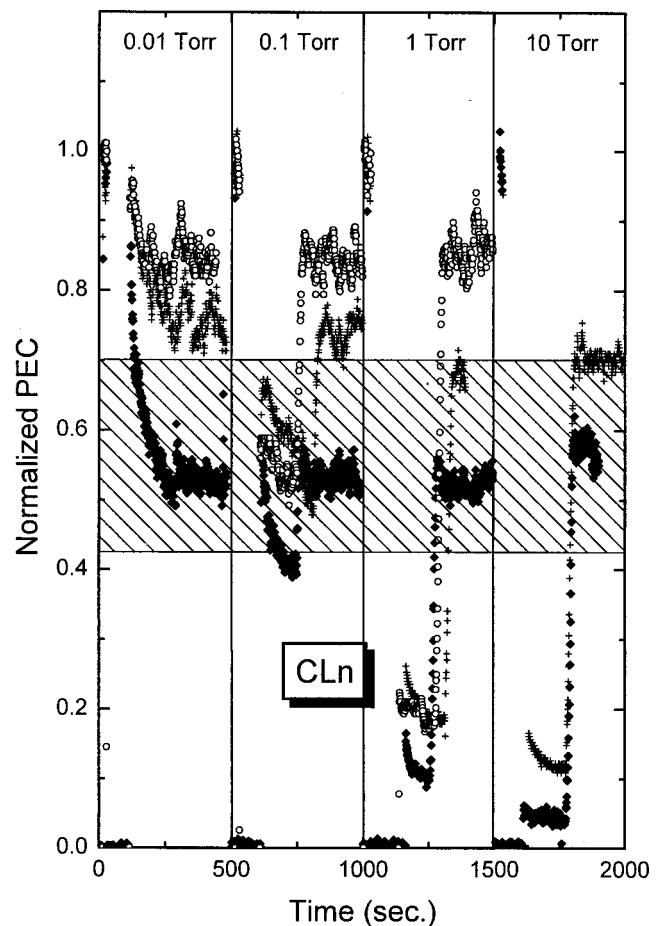


FIG. 12. Photoemission measurement sequences before, during, and after exposure to H_2 , He , and O_2 , on a CLn sample. The lined area covers the values of direct filling saturation measurements on CLn samples.

For gases other than oxygen the trends are similar to what has been found for oxygen. As can be observed in Fig. 5, the degree of current decrease in the residual current in gas specific. The CLn sample is a 15Sn sample with the oxide layer removed. Figure 6 presents the difference in residual current and the charge accumulation between the two samples for a He exposure sequence. The accumulation effect is significantly stronger for 15Sn due to increased trapping (lower residual current) and He penetration into the oxide (Fig. 2). The contribution of the oxide layer to charge trapping (having an additional family of charge traps¹) is clearly demonstrated. Figure 12 exhibits PEC exposure sequences for various pressures for O_2 , He , and H_2 on a CLn sample, the range of change due to the DF process is marked. Figure 13 summarizes the initial, exposure-saturation, and residual PEC on this sample, translated to work-function changes. Again the logarithmic pressure dependence of both the initial and saturation current is clear, while the residual current (reaching saturation) indicates efficient population of the charge traps. A clear structure can be observed: while the O_2 originated residual current is saturated well within the direct filling saturation range, the He originated one is saturated at the upper level of this range and the H_2 one well above it. This indicates one of two possibilities (or both): There is a fine structure within the charge traps in Si, namely

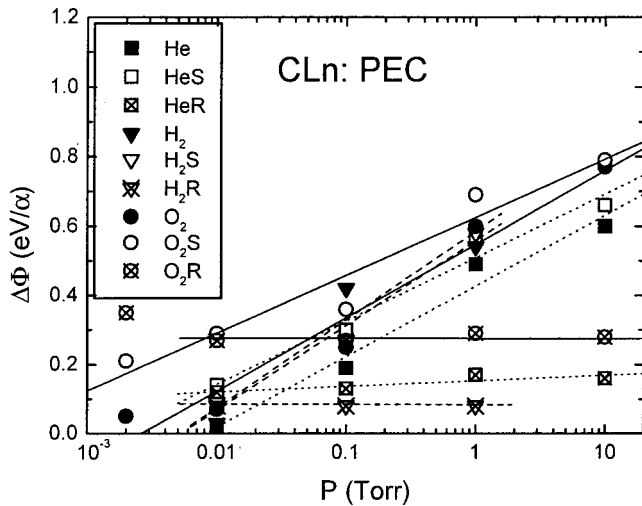


FIG. 13. Initial decrease (full), saturation under gas exposure (empty-S), and residual (dotted-R) photoemission current for He, H₂, and O₂ exposures on CLn (Fig. 12), translated to WF changes. The calibration factor is the same as in Fig. 11. The lines are best fits through the data.

not all traps are reachable by all gases and every gas can transfer PIGAC charge to a different fraction of the traps.

In addition to the trapping process, a gas-dependent detrapping process takes place, and the final residual current is a combination of the two processes. Since for H₂ there are other indications (see Figs. 8 and 9) that detrapping takes place, this possibility (reducing the number of trapped electrons—Fig. 12) agrees with that observation.

The surface charge dose is defined here as in paper I, namely the initial decrease of current (translated to $\Delta\Phi$) times the exposure time (in seconds). Here, for most gases (for which the initial decrease is approximately maintained for the whole exposure time) this definition is more meaningful. The $\Delta\Phi$ versus charge transfer dose is depicted in Fig. 14. For CO, the experimental values were very scattered (probably due to significant detrapping—see next section)

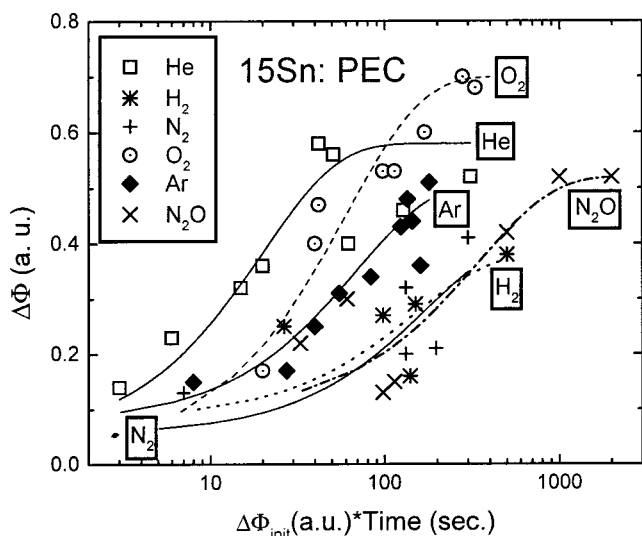


FIG. 14. The $\Delta\Phi$ (in arbitrary units) vs charge transfer dose. The lines through the experimental points are best fits to $\Delta\Phi = -A \exp(-t/\tau)$, with the values of Fig. 1.

TABLE I. Time constants and amounts of charge transfer for the different gases.

Parameter	He	H ₂	N ₂	O ₂	Ar	N ₂
τ (s)	20	147	172	60	69	340
A (a.u.)	0.53	0.30	0.35	0.68	0.43	0.53

and no trend could be deduced, so they are not shown. The lines are exponential decay fits to the experimental points (for each gas) according to $\Delta\Phi = -A \exp(-t/\tau)$. Table I presents the time constant, τ , and the amount (translated to $\Delta\Phi$) of the charge transfer, A .

Although the points are somewhat scattered (probably due to the initial diversity in trap population and detrapping) an exponential-decay dependence on the surface charge dose, expected for filling of a finite quantity of charge traps, fits quite well. He, O₂, and Ar (in this order) seem to be much more efficient than the other gases, the least effective being N₂O, although its accumulated charge transfer is relatively high. He is the most efficient (shortest time constant, although the population for O₂ reaches a higher value), probably due to its penetration into the oxide producing a significantly larger effective charged surface from which charge is transferred to traps. Oxygen, on the other hand, induces an accumulation of charge on the surface (due to the supposedly longer life of the charge on the surface in the form of O₂⁻, see paper I) creating a high charge density, a fraction of which is transferred to traps. For Ar the reason for efficiency may be that its size is relatively small (compared to the two atom molecules), enabling improved accessibility to the surface microstructure and hence to near surface charge traps. In this context, it is consistent that the efficiency of the three other molecules, H₂, N₂, and N₂O, decreases with increasing size.

C. Detrapping

In paper I, two kinds of charge dissipation from traps were observed: (a) detrapping in vacuum mainly in the sample that was partially etched in HF (HFSn) and (b) an effect (small at room temperature but much larger at 200 K) of oxygen-induced detrapping when the laser beam is off. The vacuum detrapping is believed to be caused by the thinner and damaged oxide layer, having an enlarged effective surface that brings most of the traps to the interface of either the vacuum or the Si. The gas-induced effect is probably due to the interaction of the gas molecules (either adsorbed or in the gas phase) with traps that lie close to the surface.

Some of the gases more effectively induce detrapping than others. CO, for example, induces it (in variable amplitudes) for every exposure, so no measurement of trapping residual current could be conducted (and therefore not shown in Fig. 14). A possible reason for the distinction of CO as the most efficient detrapping agent may be its polarity, but the actual mechanism is not known. Also H₂ induces detrapping in some of the exposures as can be observed in Fig. 8. When the temperature is lowered to 200 K, strong detrapping is observed (Fig. 9). This is obvious in the first three sequences (a–c), where the current increases instead of decreasing. Af-

ter the exposure to 1 Torr, the detrapping process seems to be exhausted, resulting in a significantly higher initial PEC, but an exposure sequence without detrapping. It is believed that the $\Delta\Phi$ induced by the H_2 gas-assisted charging, displayed in Fig. 14 (where only residual PEC of H_2 exposure sequences in which the detrapping effect is not obvious were considered), is a combination of trapping and detrapping. This conclusion results from the longer time constant for H_2 (147 s) as compared to Ar (69 s) though their molecular size is about the same.⁸ As mentioned before, this assumption is also consistent with the relatively reduced level of trapping for H_2 as depicted in Figs. 12 and 13. The exposure of the sample to either CO or H_2 , following gas pumpout in a PEC measurement sequence [similar to the 300 K sequence of Fig. 8(b) of paper I], did not result in enhanced detrapping compared to oxygen. For example, with He the identical 200 K and 300 K exposure plus illumination sequences support the suggestion that He is an inefficient detrapping agent.

The mechanism of either vacuum or gas-induced charge detrapping is not well understood. Also, there is no clear explanation why CO and H_2 are more efficient agents for this process than the other gases. The fact that a lower temperature increases the detrapping points to a mechanism of trap-gas interaction that increases with the decreasing distance between them, thus increasing with the increasing surface lifetime of the gas species for 200 K.

V. SUMMARY AND CONCLUSIONS

In preliminary work⁶ photoinduced gas-assisted charging was established as a general phenomenon for all gases studied, supposedly involving the electrostatic coupling of the internally photoemitted electrons with the adsorbed gas. Measurements have been extended here to additional samples (*p*-type doping and clean Si) and one gas— N_2O . It has been demonstrated for He and H_2 that charging is not restricted to the laser-irradiated spot and spreads on the surface of the oxide. The transiently trapped photoemitted electrons spread coupled to the ad-species, probably due to the Coulomb repulsion.

In the first paper in the series¹ it was demonstrated that charge transfer to traps occurs by the direct filling process in vacuum, and is enhanced by transfer of gas-assisted surface charge to direct filling as well as gas-sensitive traps in ambient oxygen. Their trap filling was shown to exist for all studied gases. The trapping saturation is gas dependent, either due to different trap availability for different gases or, more plausibly, a combination of trapping and detrapping.

Analysis of trapping efficiency shows that He is the most efficient of the gases, probably due to its small size that enables a close approach to oxide traps and penetration into the oxide (Fig. 2). This penetration creates a larger effective surface, enhanced gas-assisted charging (Fig. 1), and thus more surface electrons transferred to traps. O_2 is the second best due to the higher surface charge density formed by the accumulation of O_2^- charge. For the remaining gases it seems that the relevant parameter is the molecular (or atomic for Ar) size. This points to a possible mechanism of efficiency dependence on physical proximity to the oxide traps.

Detrapping occurs along with photo-induced gas-assisted charging, particularly for CO (its polarity may be a factor) and for H_2 . The reasons why these two gases are efficient detrapping agents while He is very inefficient is not yet clear. The physical proximity to full traps seems to also be a factor in detrapping since 200 K detrapping is much more efficient than that at 300 K, both for O_2 (paper I) and H_2 , probably due to the longer lifetime of adsorbed or gas-phase molecules at the surface.

In preliminary measurements similar photo-induced gas-assisted charging and trap filling has been observed on oxide-covered Si (111) and on oxide-covered polycrystalline molybdenum. It appears that this phenomenon is quite general, the existence of which remains to be confirmed on other systems, including clean metals.

ACKNOWLEDGMENTS

We gratefully acknowledge financial support from the Natural Sciences and Engineering Research Council of Canada and the Killam Program of the Canada Council for HMVD. We have benefitted from many useful discussions with J. G. Mihaychuk.

¹N. Shamir, J. G. Mihaychuk, and H. M. van Driel, *J. Appl. Phys.* **88**, 896 (2000).

²See, for example, D. P. Woodruff and T. A. Delchar, *Modern Techniques of Surface Science*, 2nd ed. (Cambridge U.P., Cambridge, 1994), Chap. 7.5.

³J. Oudar, in *Physics and Chemistry of Surfaces* (Blackie, Glasgow, 1975), Chap. 4.

⁴J. G. Mihaychuk, N. Shamir, and H. M. van Driel, *Phys. Rev. B* **59**, 2164 (1999).

⁵J. Bloch, J. G. Mihaychuk, and H. M. van Driel, *Phys. Rev. Lett.* **77**, 920 (1996).

⁶N. Shamir, J. G. Mihaychuk, H. M. van Driel, and H. J. Kreuzer, *Phys. Rev. Lett.* **82**, 359 (1999).

⁷P. J. Caplan, E. H. Poindexter, and S. R. Morrison, *J. Appl. Phys.* **53**, 541 (1982).

⁸J. Koresh and A. Soffer, *J. Chem. Soc., Faraday Trans. I* **76**, 2472 (1980).